MICROWAVE AND ELECTRICAL PROPERTIES OF Co–Ti SUBSTITUTED Ba–Sr FERRITE

CHARANJEET SINGH, S. BINDRA NARANG, I. S. HUDIARA, K. SUDHEENDRAN*, K. C. JAMES RAJU*, KONSTANTIN N. ROZANOV**

Department of Electronics Technology, Guru Nanak Dev University Amritsar, Punjab, India
**School of Physics, University of Hyderabad, Andhra Pradesh, India*
***Institute for Theoretical and Applied Electromagnetics, Russian Academy of Sciences, Russia*

E-mail: charanjeet2003@rediffmail.com

Submitted December 28, 2009; accepted April 07, 2010

Keywords: Ferrites; Complex Permittivity; X-Band; Resistivity

The electromagnetic parameters of synthesized M-type hexagonal ferrite, $Ba_{0.5}Sr_{0.5}Co_xTi_xFe_{(12-2x)}O_{19}$ (x = 0.0, 0.2, 0.4, 0.6, 0.8, 1.0), are measured from 8.2-12.4 GHz. The substitution of Co^{2+} and Ti^{4+} ions increases dielectric loss in the ferrite, suggesting for EMI shielding applications. The preferential site occupancy of substituted ions changes resistivity of ferrite. The various mechanisms behind variations of investigated parameters are discussed in this paper.

INTRODUCTION

The rapid development in technological applications has produced hazard in the form of Electromagnetic Interference (EMI). Hexagonal ferrites are utilized as microwave absorbers to control this environmental pollution [1]. Researchers endeavor to combat the pollution with increased magnetic losses through resonance [2-4]. However, enhanced dielectric losses in ferrites can also reduce unwanted EMI.

We reported in previous paper the static properties of Co-Ti substituted Ba-Sr hexagonal ferrite [5]. In this communication, we have investigated complex permittivity, complex permeability and resistivity of Co–Ti substituted Ba-Sr hexagonal ferrite for the first time and their possibility for high frequency application is discussed.

EXPERIMENTAL

Samples of M-type $Ba_{0.5}Sr_{0.5}Co_xTir_xFe_{(12-2x)}O_{19}$ hexagonal ferrite (x = 0.0, 0.2, 0.4, 0.6, 0.8, 1.0) are synthesized by standard ceramic method [6]. The required powders were grounded in an agate pestle and mortar for 8 hours and presintered at 1000°C for 8 hours in an electric furnace. The mixtures were then grounded again to a very fine powder under the same conditions. Sieving was carried out after the addition of polyvinyl alcohol (PVA) as binder. The mixtures were pelletized using hydraulic press under uniaxial pressure of 75 KNm^{-2}. The final sintering was performed at 1250°C for 20 hours. Slow heating and cooling rates were maintained at ± 2°C/minute.

The complex permeability (μ*) and complex permittivity (ε*) are measured with network analyzer (Agilent 8722ES) at 8.2-12.4 GHz using Nicholson-Ross method [7]. Two-Probe method is adopted to measure resistivity using Keithley setup 6517A [8].

Calibration of the analyzer was made in air before carrying out measurements, 201 sampling points were taken in the entire frequency region of interest, i.e., readings were taken with successive increment (minimum resolution) of 0.021 GHz.

The corresponding scattering matrix parameters in a two port network are calculated as [7]

$$S_{11} = \frac{\Gamma(1-T^2)}{(1-\Gamma^2T^2)} \quad (1)$$

and

$$S_{21} = \frac{T(1-\Gamma^2)}{1-\Gamma^2T^2} \quad (2)$$

where Γ is the reflection coefficient, and T is the transmission coefficient. These parameters can be read from the network analyzer. The reflection coefficient can be deduced as

$$\Gamma = X - \sqrt{X^2-1} \quad (3)$$

$|\Gamma| < 1$ is used to find the exact root of this equation, which is

$$X = \frac{S_{11}^2 - S_{21}^2 + 1}{2S_{11}} \quad (4)$$

The transmission coefficient is

$$T = \frac{S_{11} + S_{21} - \Gamma}{1-(S_{11} + S_{21})\Gamma} \quad (5)$$

The complex permittivity is then can be calculated as

$$\varepsilon^* = \frac{\lambda_0^2}{\mu}\left\{\frac{1}{\lambda_c^2} - \left[\frac{1}{2\pi L}\ln\left(\frac{1}{T}\right)\right]^2\right\} \quad (6)$$

where L is the thickness of the sample.

The complex permeability is calculated as

$$\mu^* = \frac{1+\Gamma}{\Lambda(1-\Gamma)\sqrt{\frac{1}{\lambda_0^2} - \frac{1}{\lambda_c^2}}} \quad (7)$$

where λ_0 is the free space wavelength and λ_c is the cut-off wavelength, and

$$\frac{1}{\Lambda^2} = \left[\frac{1}{2\pi L}\ln\left(\frac{1}{T}\right)\right]^2 \quad (8)$$

RESULTS AND DISCUSSION

Complex Permittivity, Resistivity and Complex Permeability

Dielectric constant (Figure 1a,b) of all samples exhibits non-linear variation with substitution of Co^{2+} and Ti^{4+} ions; this behavior is neither resonance nor relaxation type. In our previous investigation, substitution of Co^{2+} and Ti^{4+} ions caused non-homogeneous structure, increase in grain size, density and reduction in grain boundaries [5]. Large porosity and low density reduces dielectric constant and dielectric loss [9]. High resistivity discourages polarization and conductivity. Resistivity increases at x = 0.2 (279×10^3 Ωcm) and decreases thereafter (Table 1). Thus combined effect of resistivity and porosity causes non-linear variation of dielectric properties with substitution.

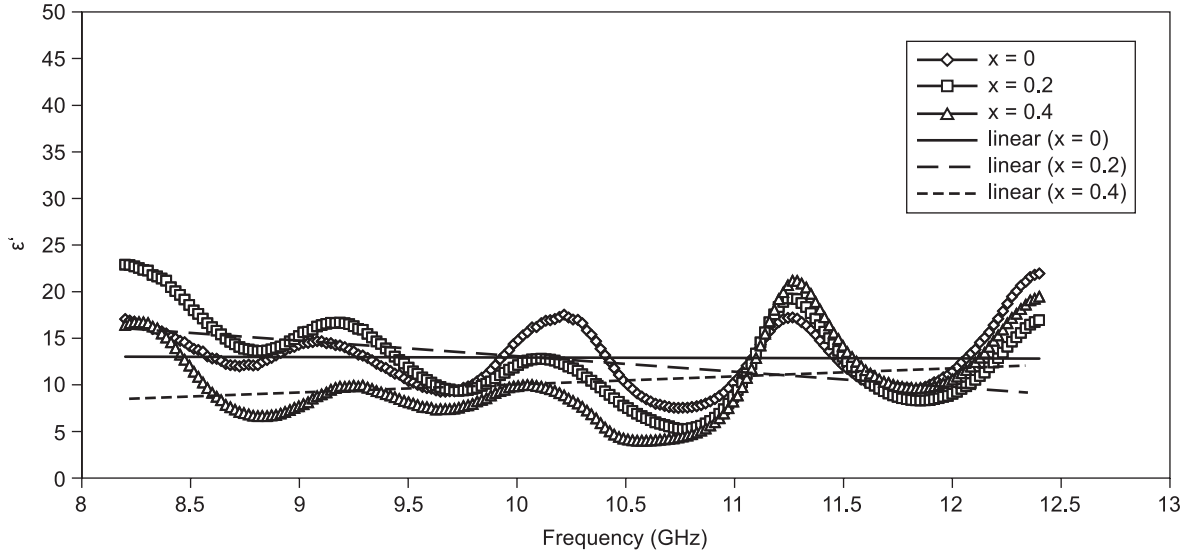

a) x = 0.0, 0.2, 0.4

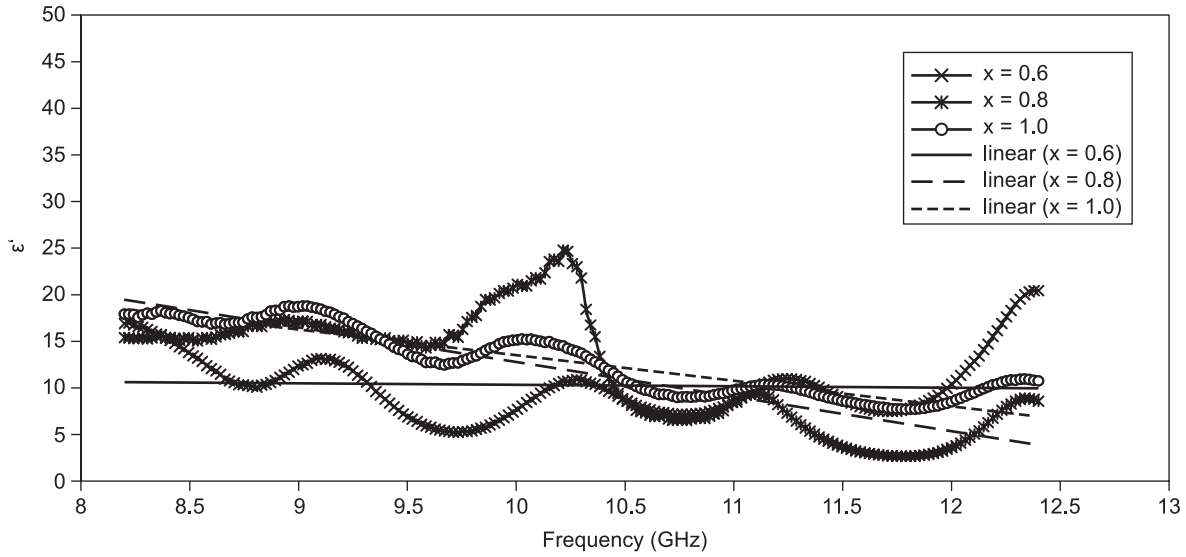

b) x = 0.6, 0.8, 1.0

Figure 1. Dielectric constant variation of $Ba_{0.5}Sr_{0.5}Co_xTi_xFe_{(12-2x)}O_{19}$ ferrite as a function of frequency and substitution.

Dielectric constant in ferrites depends on space charge polarization and charge formation at the grain boundaries. It has been reported elsewhere that electron hopping between Fe^{2+} ions and Fe^{3+} ions leads to conductivity and dielectric polarization in ferrites [10]. Researchers have reported the formation of Fe^{2+} ions from Fe^{3+} ions at high temperature synthesis of ferrites [11-15]. The temperature plays important role in deciding dielectric properties of synthesized ferrite. At low temperature, the bound charge carriers are not able to align in the direction of applied field. This contributes to weak polarization, hence, dielectric properties. However charge carriers are excited through thermal energy at high temperature and follow the changes in applied field, enhancing dielectric properties through polarization [16]. Thus large ε' and ε'' in all samples is due to formation of Fe^{2+} ions from Fe^{3+} ions at sintering temperature of 1250ºC. This high temperature causes increase in electron hopping between Fe^{2+} ions and Fe^{3+} ions.

Table 1. Resistivity of $Ba_{0.5}Sr_{0.5}Co_xTi_xFe_{(12-2x)}O_{19}$ ferrite.

x	ρ (Ωcm)
0	105×10^3
0.2	279×10^3
0.4	72×10^3
0.6	75×10^3
0.8	74×10^3
1.0	72×10^3

Undoped sample 0.0 possesses large ε' and ε'' in spite of having highest porosity [5] and high resistivity of 105×10^3 Ωcm (Table 1): pores offer hindrance to electron flow. Sample 0.0 has maximum number of Fe^{3+} ions available for conversion to Fe^{2+} than doped samples,

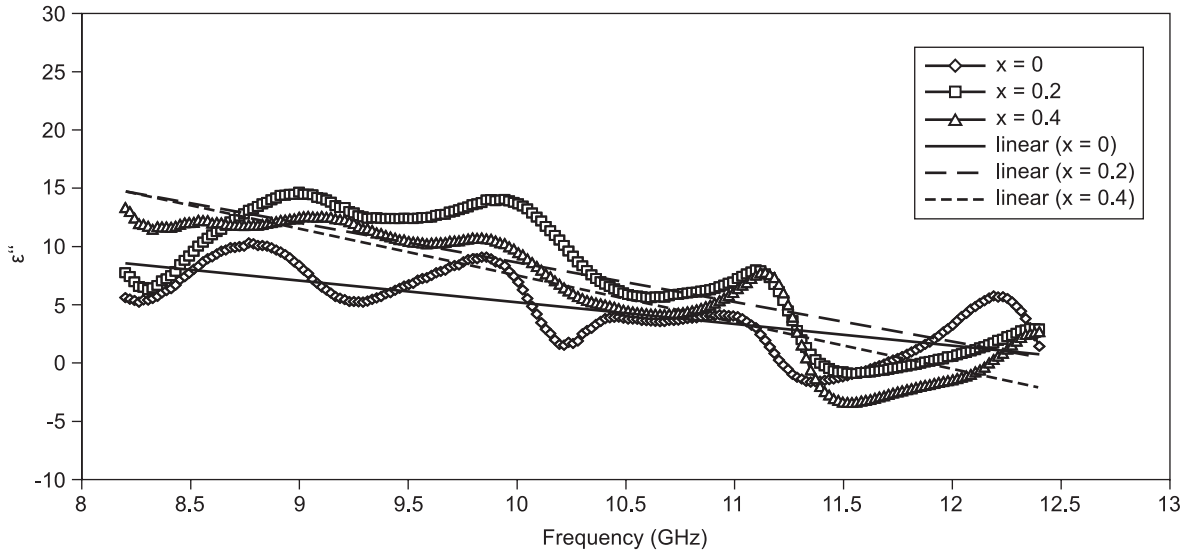

a) x = 0.0, 0.2, 0.4

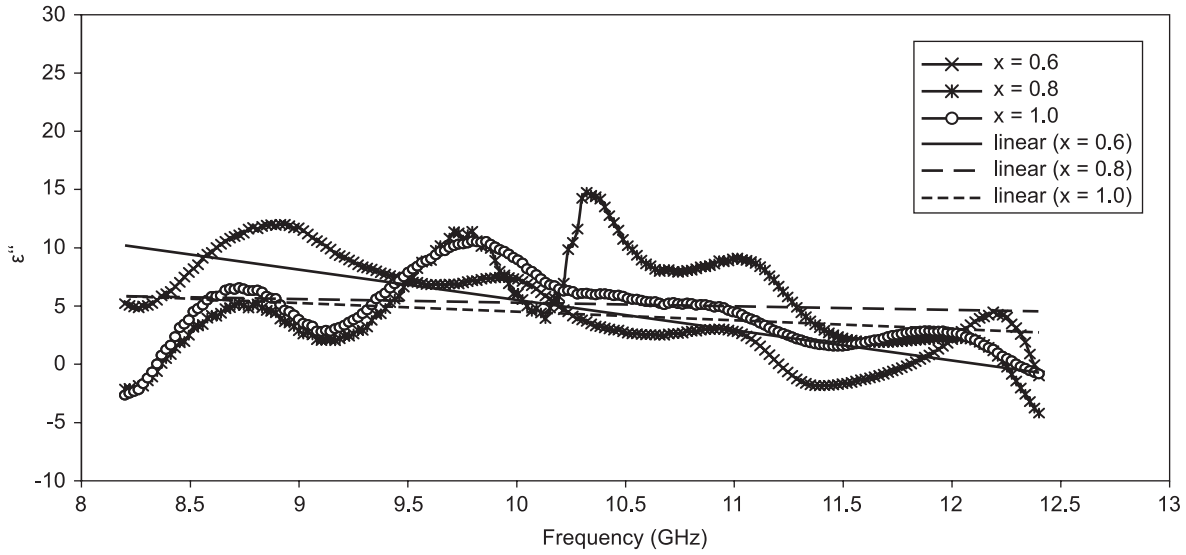

b) x = 0.6, 0.8, 1.0

Figure 2. Dielectric loss variation of $Ba_{0.5}Sr_{0.5}Co_xTi_xFe_{(12-2x)}O_{19}$ ferrite as a function of frequency and substitution.

so large number of Fe^{2+} ions are produced from Fe^{3+} ions. Thus polarization is enhanced resulting in increase of both ε' and ε'' in sample 0.0.

Figure 3 exhibits microstructure of undoped sample 0.0 and doped sample 1.0. The porosity and strength of grains is reduced with substitution as observed in sample 1.0. The substitution of Co^{2+} and Ti^{4+} ions improves grain connectivity encouraging the polarization, thus, dielectric properties. However, undoped sample 0.0 exhibits large ε' and ε'' besides owing large number of grains and intergranular pores. As discussed before, it is attributed to availability of maximum number of Fe^{3+} ions for conversion to Fe^{2+} ions at 1250°C for electron hopping.

In M-type hexagonal ferrite, Fe^{3+} cations occupy seven octahedral sites 12k and 2a, trigonal site 2b with spin in one direction, while two tetrahedral sites 4f1 and two octahedral sites 4f2 have spin in opposite directions [17]. Thus resistivity in ferrites depends on octahedral site (B) and this site is large than tetrahedral site (A) [18]. Ligand theory describes dependence of site occupancy on d-configuration and nature of other partner cation [19]. The electronegativity for Ti^{4+} ions is higher than that of Co^{2+} ions, thus former ions can occupy octahedral site. The Co^{2+} ions prefer to occupy octahedral site with d^7 configuration and Ti^{4+} ions have no site preference due to d^0 configuration. Zhou et al. reported that Co-Ti ions strongly prefer 2b and 4f2 sites [20] while Batlle et al. reported Ti^{4+} ions for 4f2 site [21]. Kalvoda et al. reported that both Co^{2+} and Ti^{4+} ions can occupy 12k and 4f2 sites while alone Co^{2+} prefer 4f1 sites [22]. The Co^{2+} ions may also occupy octahedral site on the account of large ionic radius (0.72 Å) than Ti^{4+} ions (0.68 Å) [5].

The preferential occupancy described above of substituted Co^{2+} and Ti^{4+} ions displaces Fe^{3+} ions from B to A sites, it increases resistivity at lower substitution. Further substitution increases number of Fe^{3+} ions displacement which in turn increases the electron hopping between Fe^{2+} and Fe^{3+} ions. Thus further substitution causes reduction in resistivity due to increased electron hopping. Another reason associated with this variation is the preferential occupancy Co^{2+} ions for A-sites in addition to B-sites [23]. It will result in displacement of Fe^{3+} ions from A to B sites apart from B to A sites as discussed before. Thus net displacement of Fe^{3+} ions from B to A site will less than that of lower substitution, causing resistivity to decrease with further substitution.

Resistivity is also influenced by microstructure in addition to site occupancy of ions. The microstructure in Figure 3 shows decrease in grain boundaries with substitution. These grain boundaries impede domain wall motion, so grain boundaries offer resistivity [24]. Thus high resistivity in undoped sample 0.0 can be due to large number of grain boundaries present in it. Similar reason applies for sample 1.0 with lowest value of resistivity due to small number of grain boundaries present in it.

The complex permeability exhibits oscillatory behavior similar observed in complex permittivity. However, it does not convey any significant variation to be discussed in this investigation.

Oscillatory Behavior of ε* and μ*

The hexagonal ferrites manifest an oscillatory behavior in their dielectric and magnetic properties. Meshram et al. reported the electromagnetic properties of Ba–Co and Ba–Mn– at X-band [25]. The samples

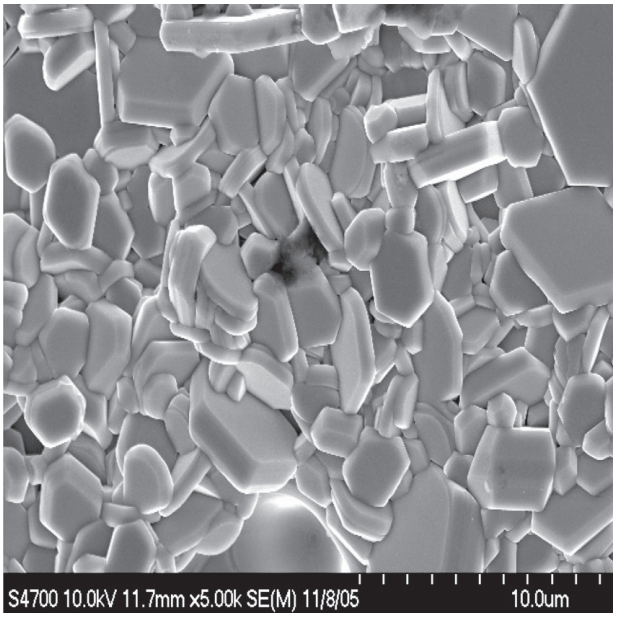

a) x = 0

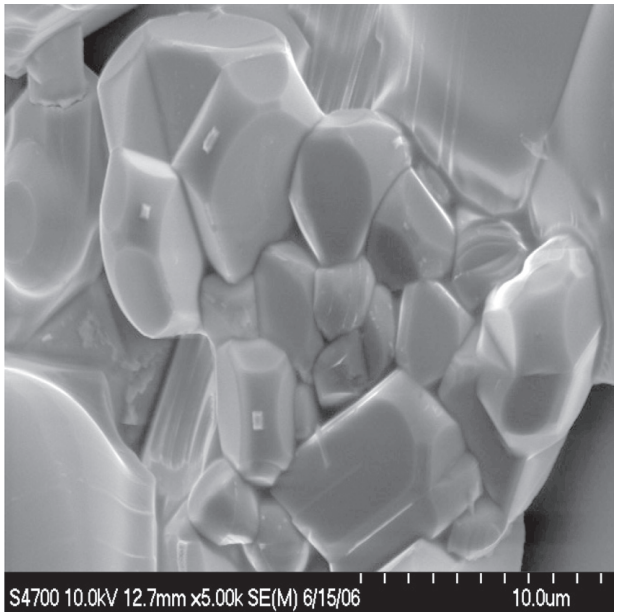

b) x = 1

Figure 3. SEM micrographs of $Ba_{0.5}Sr_{0.5}Co_xTi_xFe_{(12-2x)}O_{19}$ ferrite.

exhibited the oscillatory behavior for dielectric as well as magnetic properties. Abbas et al. [26] also described similar oscillatory behavior in complex permittivity and permeability of substituted M-type Ba Hexagonal ferrites. The oscillatory mechanism in dielectric properties was attributed to difference in relaxation frequencies of various dipoles and magnetic properties were dependent on interaction of the magnetic vector with microwave signal, and the change in direction of the magnetization vector with substitution.

Ferrites consist of various positive ions with different valencies and have different co-ordination with O^{2-} ions reported by Abbas at el. [26]. This forms dipoles of different strengths in the ferrite and these different dipoles have different relaxation frequencies. The electron hopping between Fe^{2+} and Fe^{3+} ions will give rise to another relaxation. Therefore different relaxation mechanisms of various dipoles formed, electron hopping and relaxation characteristics associated with space charge polarization altogether are the presumable factors responsible for oscillatory behavior of the dielectric properties.

The oscillations in complex permeability can be explained in terms of the precision motion of the magnetization vector. In M-type hexagonal ferrites the 12 Fe^{3+} ions occupy positions in three different interstitial sites viz. tetragonal, octahedral and bi-pyramidal. The seven octahedral ions and one bi-pyramidal ion have up-spins while two octahedral ions and two tetrahedral ions have down-spins giving net magnetization of only 4 Fe^{3+} ions. The magnetization vector should produce stable resonances on interaction with microwave signal. But magnetization vector will be inclined more towards the base line after the substitution of Co^{2+} and Ti^{4+} ions and its interaction with the microwave signal results in oscillatory behavior of the magnetic properties. Referring to Figures 1-2, it could be stated that the sample responses vary with the frequency and substitution, other parameters like sample thickness and measurement conditions are same for all the samples.

Moreover, a slight oscillation in the measured data is possible from the measurement procedure itself. It is known that the Nicholson Ross method, adopted to find complex permittivity and permeability, shows a divergence at frequencies corresponding to integral multiples of half wavelength in the sample. In this investigation, complex transmission (T) and reflection coefficient (Γ) are calculated from S-parameter measurements. Nicholson and Ross assumed an infinitely thick sample taking into consideration the behavior of reflection coefficient. Reflection coefficient is a oscillatory function of sample thickness with periodic oscillations at every half wavelength [27]. In the case of absorbing materials, the amplitude of oscillation increases with the reduction in sample thickness. When the sample is infinitely thick, the refection coefficient becomes constant. In the present investigation, the Nicholson Ross method was used to calculate the T in terms of measured Γ, complex permittivity and complex permeability. This method cannot rule out the effect of oscillatory behavior of the complex reflection coefficient (Γ) in the dielectric and magnetic properties until the sample is of finite thickness.

The Figure 4 shows that dielectric loss is in anti-

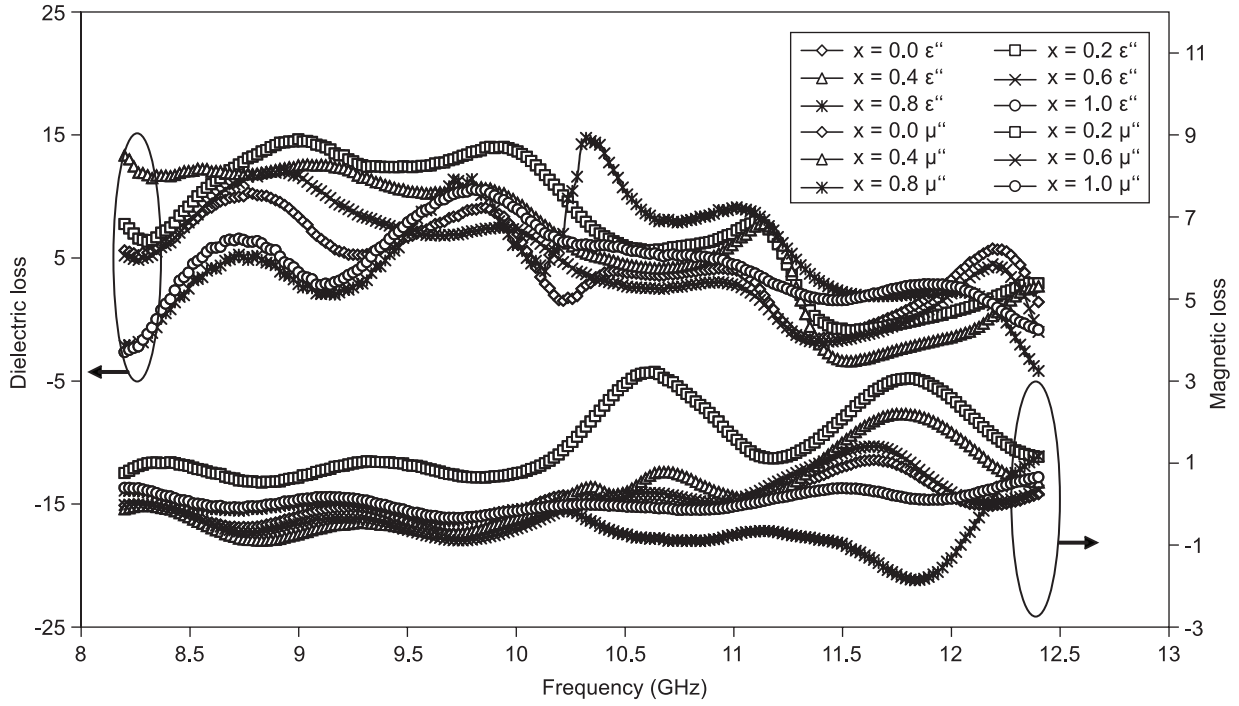

Figure 4. Anti-phase oscillations of μ'' and ε'' in $Ba_{0.5}Sr_{0.5}Co_xTi_xFe_{(12-2x)}O_{19}$ ferrite (x = 0.0,0.2,0.4,0.6,0.8,1.0).

phase oscillations with magnetic loss from 8.2 GHz to 12.4 GHz. Thus the total loss (dielectric + magnetic) does not oscillate with frequency, concluding that oscillations in μ'' and ε'' (also in μ' and ε') are due to measurement uncertainty and apparent splitting is ascribed to the measurement error. Negative values in μ' (X-Band) have also been reported elsewhere [28-29].

Consequently, oscillatory behavior in investigated electromagnetic parameters can be attributed to combined behavior of the material properties and the measurement procedure itself.

CONCLUSIONS

1. This first ever investigation on Co–Ti substituted Ba–Sr ferrites concludes that microwave attenuation is also governed by increased dielectric losses through appropriate sintering temperature and substitution. In previous investigations, magnetic properties are enhanced to achieve microwave attenuation.
2. Increased hopping mechanism at high sintering of 1250°C accompanied by microstructural properties and resistivity variation account for enhancement of ε' and ε''.
3. The preferential site occupancy of Co^{2+} and Ti^{4+} ions increases resistivity to 279×10^3 Ω.cm in sample 0.2.
4. The significant dielectric loss indicates the possible use of these materials for EMI shielding application at X-Band.

References

1. Inui T., Oda K.: IEEE Trans. Magn. *35*, 3148 (1999).
2. Pardavi-Horvath M.: J. Magn. Magn. Mater. *215-216*, 171 (2000).
3. Cho H. S., Kim S. S.: IEEE Trans. Magn. *35*, 3151 (1999).
4. Verma A., Mendiratta R. G., Goel T.C., Dube D.C.: J. Electroceram. *8*, 203 (2002).
5. Singh C., Bindra Narang S., Hudiara I.S., Bai Y., Marina K.: Mat. Let. *63*, 1921 (2009).
6. Goldman A. J.*: Handbook of Modern Ferromagnetic Materials*, Kluwer Academic Publishers, 1999.
7. Nicolson A. M., Ross G. F.: IEEE Trans. Instrum. Meas. IM-19, 377 (1970).
8. Murthy V. R. K. and Sobhanadri J.: Phys. Status. Solidi A *38*, 647 (1976).
9. Mangalraja R. V., Ananthakumar S., Manohar P., Gnanam F.D.: Mat. Let. *57*, 1151 (2003).
10. Abdeen A. M.: J. Magn. Magn. Mater. *192*, 121 (1999).
11. Gupta N., Dimri M. C., Kashyap S. C., Dube D. C.: Ceram. International *31*, 171 (2005).
12. Van Uitert L. G.: J. Chem. Phys. *23*, 883 (1955).
13. Verma A. and Chatterjee R.: J. Magn. Magn. Mater. *306*, 313 (2006).
14. Brownlow J.M.: J. Appl. Phys. *29*, 373 (1958).
15. Bao J., Zhou J., Yue Z., Li L., Gui Z.: J. Magn. Magn. Mater. *250*, 131 (2002).
16. Anantharaman M. R., Sindhu S., Jagatheesan S., Molini K. A., Kurian P.: J. Phys. D: Appl. Phys. *32*, 1801 (1999).
17. Lisjak D., Drofenik M.: J. Eur. Cer. Soc. *24*, 1841 (2004).
18. Rane M. V., Bahadur D., Kulkarni S. D., Date S.K.: J. Magn. Magn. Mater. *195*, L256 (1999).
19. González-Angeles A., Mendoza-Suárez G., Grusková A., Lipka J. and Papánová M., Sláma J.: J. Magn. Magn. Mater. *285*, 450 (2005).
20. Zhou X. Z., Morrish A. H., Li Z. W. and Hong Y. K.: IEEE Trans. Magn. *27*, 4654 (1991).
21. Batlle X., Obradors X., Pernet M., Vallet M., Cabanas M., Rodriguez and Fontcuberta J.: J. Magn Magn. Mater. *83*, 465 (1990).
22. Kalvoda L., Dlouha M., Vratislav.: J. Magn. Magn. Mater. *87*, 243 (1990).
23. Šimša Z., Lego S., Gerber R. and Pollert E.: J. Magn. Magn. Mater. *140–144*, 2103 (1995).
24. Zahi S., Hashim M. and Daud A. R.: J. Magn. Magn. Mater. *308*, 177 (2007).
25. Meshram M.R., Agrawal N.K., Sinha B., Misra P.S.: J. Magn. Magn. Mater. *71*, 207 (2004).
26. Abbas S. M., Dixit A. K., Chatterjee R., Goel T. C.: J. Magn. Magn. Mater. *309*, 20 (2007).
27. Abbas Z., Pollard R. D., Kelsall R. W.: IEEE Trans. Microwave Theory Tech. *46*, 2011 (1998).
28. Brown F., Gravel C. L.: J. Phys. Rev. *97*, 55 (1955).
29. Von Aulock W. H.: *Handbook of Microwave Ferrite Materials*, Academic Press, London, 1965.